

Neutrino-induced multilepton events arising from the associated production of charmed particles

G. L. Kane

Physics Department, The University of Michigan, Ann Arbor, Michigan 48109

J. Smith

Institute for Theoretical Physics, SUNY at Stony Brook, Stony Brook, New York 11794

J. A. M. Vermaseren

Department of Physics, Purdue University, West Lafayette, Indiana, 47907

(Received 28 July 1978)

We discuss the contribution of associated production of charmed pairs $c\bar{c}$ to multilepton events in ν reactions, with emphasis on like-sign dimuons and trimuons. Both absolute rates and constraints from distributions are considered. We give one treatment which is purely phenomenological, obtaining the maximum amount of $c\bar{c}$ production which can be consistent with existing data on distributions, and giving relative amounts for different multilepton states. We also attempt a theoretical analysis which gives an estimate for the magnitude of $c\bar{c}$ production in ν reactions starting from photoproduction of ψ ; this leads to a rate significantly larger than that due to perturbative quantum-chromodynamics estimates made so far. We give results for both the 350-GeV wide-band neutrino beam at CERN and the 400-GeV quadrupole triplet neutrino beam at Fermilab, including experimental cuts. Our results for trimuons and dimuons arising from $c\bar{c}$ decays are that $\sigma(\mu^-\mu^-\mu^+)/\sigma(\mu^-) \lesssim 1 \times 10^{-5}$ and $\sigma(\mu^-\mu^-)/\sigma(\mu^-\mu^+) \lesssim 2 \times 10^{-2}$. We do not find any need to search for anomalous sources of multimueon events.

I. INTRODUCTION

The single excitation of charmed particles in neutrino interactions is in excellent agreement with the predictions of the Glashow-Iliopoulos-Maiani (GIM) model.¹ Recent analysis of dimuon data by the CERN-Dortmund-Heidelberg-Saclay (CDHS) group² has shown that the $x=Q^2/2M\nu$ distribution for sea quarks behaves like $(1-x)^7$. Odorico³ and Lai⁴ have used data from the CDHS group and the Columbia-Brookhaven (CB) group⁵ to examine the behavior of the fragmentation function for charmed particles. This function seems to fall off slower than the corresponding function used to describe the production of pions. Hadronic production data by neutrinos and antineutrinos is being analyzed by many groups. With enough events, one can reconstruct invariant masses and, it is hoped, see the D and F mesons.⁶

In contrast, the situation regarding the associated production of charm is presently very poor. The discovery of trimuon events at Fermilab by the Caltech-Fermilab (CF) group⁷ and the Fermilab-Harvard-Pennsylvania-Rutgers-Wisconsin (FHPRW) group⁸ together with the CDHS events⁹ at CERN should shed some light on associated charm production because such events arise when the hadronic particles containing the charmed quarks decay semileptonically. Indeed, just after the publication of the first trimuon events, Bletzacker, Nieh, and Soni¹⁰ proposed that they are

manifestations of associated charm production. These authors constructed a phenomenological model similar in spirit to a previous model used to discuss the $c\bar{c}$ interpretation of multimueon events produced in muon beams¹¹ in which they assumed a diffractive-dissociation character (small x) for the production process. At that time the neutrino data was very limited so the authors could not make a detailed evaluation of their model. However, they made several predictions for the rates and distributions for trimuon events and same-sign dimuon events (which arise when one charmed particle decays via a semileptonic mode and the other decays via a hadronic mode). Significantly more data is now available on these channels.^{12,13,14} Bletzacker *et al.* did not give any normalization of the trimuon rate on a dynamical level, i.e., based, for example, on the theory of quantum chromodynamics but invoked the conserved-vector-current hypothesis to relate the W -boson production of dimuons to the analogous production via virtual photons. However, this is not reliable since only the isoscalar part of the photon is involved in $\gamma \rightarrow c\bar{c}$. Later Goldberg¹⁵ and Young, Walsh, and Yang¹⁶ made calculations of $c\bar{c}$ production based on gluon bremsstrahlung from valence quarks in the proton (or isoscalar target). In these calculations the absolute magnitude of associated $c\bar{c}$ production was determined. Unfortunately, the trimuon and dimuon rates were too small to be of importance experimentally, so

these authors did not present any trimuon distributions in a form where they could be directly compared with the data. There is therefore a lack of information in the literature on trimuon distributions arising from $c\bar{c}$ production off valence quarks.

It is now appropriate to reexamine $c\bar{c}$ production for two reasons. First, high-statistics trimuon data is already available from the CDHS experiment¹² and will soon be available from the FHPRW and CF groups. At present, the situation regarding same-sign dimuon production is not yet clear. The FHPRW group¹⁴ has reported evidence for a real signal in this channel, while the CDHS group is not so positive on this issue.¹³ However, we can compare the CDHS trimuon distributions with the predictions of models and try to work backwards to bound the possible dimuon contributions from $c\bar{c}$ production and decay. The explanation presented by the CDHS group¹² for their trimuon events does not include any explicit component arising from $c\bar{c}$ decays.

A further reason for studying $c\bar{c}$ production is that beam-dump studies¹⁷ indicate a reasonably large hadronic cross section for charmed-particle production of the order of 200 μb . Although the experiments referred to in Ref. 17 do not agree on a precise number, such a large cross section was unexpected. In addition, experimental results on the photoproduction of the J/ψ ¹⁸ can be used to estimate that the size of the inelastic cross section for charm photoproduction is around $\frac{1}{2}$ μb . This means that the inelastic cross section for charm production is approximately $\frac{1}{2}\%$ of the total γN cross section. If charmed particles are pair produced so copiously in hadronic and electromagnetic interactions, then it is reasonable to assume that there is also a large signal in neutrino interactions. We say "reasonable" because the precise nature of the underlying dynamics of charmed-particle production is not understood. While a photon can pair produce charmed quarks by its electromagnetic coupling, any connection to neutrino production via the conserved-vector-current hypothesis is rather vague.

We approach the problem of $c\bar{c}$ production in neutrino collisions from two viewpoints.

(1) As there is no accepted model, we try to work backwards from the recent trimuon data to get some limit on the size of a potential $c\bar{c}$ signal. Thus, we tentatively accept the gluon-bremsstrahlung model and use it to calculate the trimuon event rate and distributions. Although the actual rate is too low to explain the size of the trimuon signal, we have reason to believe that, given the experimental cuts, the distributions are probably roughly correct. We will then compare these distributions with the CDHS data to try to extract a

reasonable upper bound on a potential $c\bar{c}$ production cross section. We then try to correlate the $\mu^-\mu^-$ signal with the trimuon signal. The ratio of the cross sections, i.e., $\sigma(\mu^-\mu^-)/\sigma(\mu^-\mu^-\mu^+)$, does not depend on the magnitude of the $c\bar{c}$ production cross section and is a decisive test of the model. The $c\bar{c}$ explanation of the trimuon data naturally leads to a much larger $\mu^-\mu^-$ rate, so it is imperative to have a precise measurement of this quantity. We calculate the distributions for the $\mu^-\mu^-$ events and compare them with the recent FHPRW results. More data on this channel will soon be available from the CDHS group.

(2) We give an estimate of the size of associated $c\bar{c}$ production expected in ν reactions, starting from the expected cross section for photoproduction of charm, and using normally safe and checked techniques such as approximate vector dominance. This gives an estimate for $\sigma(\nu \rightarrow c\bar{c})$ independent of any assumption that certain diagrams dominate. We also can argue that in the kinematical situation under consideration, the single gluon-bremsstrahlung diagram will not dominate. The resulting estimate for $\sigma(\nu \rightarrow c\bar{c})$ is consistent with the bound obtained as described above and constitutes the best estimate we can make of the actual size of associated production of $c\bar{c}$ in ν reactions.

The plan of the paper is as follows. In Sec. II we present some model-independent estimates for charm production. Specific dynamical models are discussed. Then in Sec. III we examine one particular model. We compare its predictions with the CDHS trimuon data in Sec. IV. Having bounded the possible magnitude of the $c\bar{c}$ component, we turn our attention to opposite- and same-sign dimuon signals in Sec. V. Finally, in the last section (Sec. VI) we give our conclusions.

II. ESTIMATE OF ABSOLUTE SIZE OF ASSOCIATED $c\bar{c}$ PRODUCTION

In this section we try to make the best estimate we can of the expected size of $c\bar{c}$ production. As discussed in the Introduction, in view of the large size of the charm-production cross section in pp reactions and photoproduction, we expect a significant amount of $c\bar{c}$ production in ν reactions. Qualitatively, we expect considerably more $c\bar{c}$ production than is obtained in Refs. 15, 16 from the assumption that the single gluon-bremsstrahlung diagram dominates.

Basically, the argument goes as follows. Consider photoproduction of ψ , $\gamma p \rightarrow \psi p$. Consider a crude unitarity argument.¹⁹ Let M be the amplitude for $\psi p \rightarrow \psi p$. Then $M \simeq i\sigma_T s e^{Bt}$, $d\sigma/dt \simeq \sigma_T^2 e^{2Bt}/16\pi$, and $\sigma_{el} \simeq \sigma_T^2/32\pi B$. Using²⁰ $B \simeq 1.5$ (GeV/c)⁻² = 0.6 mb and $\sigma_T \simeq 2$ mb, we get $\sigma_{el}/\sigma_T \simeq \frac{1}{30}$.

Next, we assume $\sigma(\gamma p \rightarrow \bar{D}C)/\sigma(\gamma p \rightarrow \psi p) \approx \sigma_T(\psi p)/\sigma_{el}(\psi p) \approx 30$, where with $\sigma(\gamma p \rightarrow \bar{D}C)$ we include also the cross sections with additional final pions. Note that since $m_\psi + m_p \approx 4 \text{ GeV}/c^2$ and $m_D + m_C \geq 4.2 \text{ GeV}/c^2$, there should be no important suppression due to masses.

Experimentally, $\sigma(\gamma p \rightarrow \psi p)$ grows with energy²⁰ over the region of interest, and a very careful calculation would include that variation. Here we use average numbers; we take $\sigma(\gamma p \rightarrow \psi p) \approx 20 \text{ nb}$. Then we obtain $\sigma(\gamma p \rightarrow \bar{D}C) \approx 600 \text{ nb}$. That is, associated production of charm by photons is expected to be about $\frac{1}{2}\%$ of the total photoproduction cross section. A similar argument for associated production of strangeness gives results consistent with experiment.

Next we must find a way to translate this into a useful estimate for ν reactions. First, we examine other work relevant to the photoproduction case. We are aware of two papers^{21,22} in which the diagrams in Fig. 1 are calculated. They obtain numerical results for photoproduction of charm which are consistent with the rigorous lower bound from unitarity or a little below it, and a factor of 3–4 less than the estimate of $\frac{1}{2}\%$ for $\sigma_T(\gamma p)$. However, the diagram of Fig. 1 takes advantage of the $c\bar{c}$ component of the electromagnetic current and does not include the effect of the gluon bremsstrahlung or Compton diagrams used in Refs. 15, 16 to calculate $c\bar{c}$ production for ν reactions. The analogous diagrams for photoproduction are shown in Fig. 2 and are also of order eg^2 in amplitude, where g is the gluon coupling constant. Therefore, we see no reason why one or the other should dominate.

Further, it is not clear why associated production of $c\bar{c}$ should be calculable perturbatively. For example, consider the diagram of Fig. 3. This has two gluons and is of order eg^4 . But one must worry about the momentum transfer at which the coupling is evaluated; for a semi-inclusive process such as $c\bar{c}$ associated production, such contributions are not included in scaling violations. Then for Fig. 3 we have $g^4(q^2)$, while for Fig. 1 we have $g^2(Q^2)$, where q and Q are the respective momentum transfers. If important contributions come from $q^2/Q^2 \sim \frac{1}{2} - \frac{1}{4}$, then assuming g^2 falls as $\ln(Q^2/Q_0^2)$, one

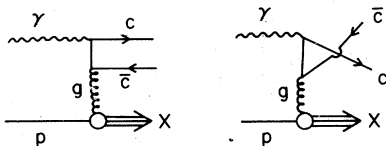


FIG. 1. Feynman diagrams for the photoproduction of a pair of charmed quarks via the one-gluon-exchange mechanism.

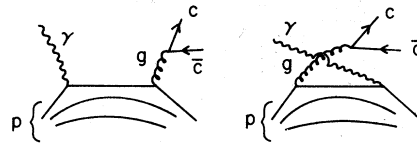


FIG. 2. Feynman diagrams for the single gluon-bremsstrahlung production of a pair of charmed quarks in photoproduction.

could find $g^4(q^2)$ comparable in size to $g^2(Q^2)$. In addition, the $c\bar{c}$ pair are produced by any of Figs. 1, 2, 3 near threshold, with small relative momenta, and for Figs. 2, 3 with small momenta relative to other final quarks, so final-state interactions involving multiple gluon exchanges are not obviously small.

There is another reason for suspecting that the mechanism depicted in Fig. 3 yields a larger cross section than that from Fig. 2. The gluon propagator in Fig. 2 is timelike and has a minimum value of $(2m_c)^2$, which is rather large and tends to suppress the resulting cross section. In contrast, the gluon propagators in Fig. 3 are spacelike and can be very small. Therefore, the situation is somewhat analogous to the case of two photon reactions versus one photon reactions in electron-positron colliding-beam experiments where, even though the two photon mechanism is suppressed by α^2 , it has a different mass scale and has the larger cross section at high energies.

We tentatively conclude, then, that photoproduction of $c\bar{c}$ proceeds by two mechanisms of comparable importance, one where the $c\bar{c}$ component of the γ is excited by gluon exchange, and the other where a struck quark radiates a gluon which pair produces $c\bar{c}$, perhaps with additional interactions. The latter process does not have one dominant Feynman diagram, but several of equal importance, all of which yield similar distributions in most variables.

Now we can make the transition to ν reactions. There is no contribution analogous to Fig. 1, since the charged W does not dissociate to $c\bar{c}$. But the

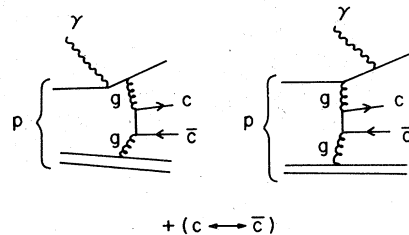


FIG. 3. Feynman diagrams for the photoproduction of charmed quark via two-gluon annihilation.

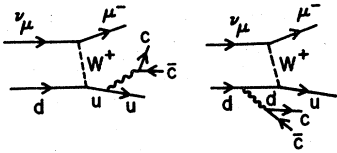


FIG. 4. Feynman diagrams for the single-gluon-bremsstrahlung production of a pair of charmed quarks in neutrino interactions.

contributions of Fig. 2 and Fig. 3 can be directly estimated. We use a vector-dominance estimate, assuming it to be valid at the factor-of-2 level or better. Now, $\gamma \sim \rho^0 + \omega^0/3 - \sqrt{2}\phi/3 + 2\sqrt{2}\psi/3$. We take the relative contribution of Figs. 2, 3 and Fig. 1 to be in the proportion of $\rho + \omega$ to ψ , giving $(9+1)/8 = 5/4$, ignoring strange quarks. Then the isovector fraction (ρ^0) of the bremsstrahlung contribution is $9/(9+1) = 9/10$. To go to the charged-current coupling there is a factor of $\sqrt{2}$ in amplitude. Thus, we estimate the amount of associated production of $c\bar{c}$ in ν reactions to be about

$$\left(\frac{1}{2}\right) \times \frac{5}{8} \times \frac{9}{10} \times 2 = \frac{1}{2}\%$$

of the total ν cross section (if associated production of charm is about $\frac{1}{2}\%$ of the total photoproduction cross section). Although we have ignored questions of coherence and various subtleties, this estimate should be a reasonable one, and is our "best" guess at the expected rate.

If this estimate is correct, then associated production of $c\bar{c}$ predicts raw multilepton rates which only depend now on the branching ratio for semileptonic decay. However, before these numbers can be compared with experiment the effects of the experimental apertures, which are very severe, must be included. This is where we are forced to assume a more specific model because we need to know the energy and angle spectra of the c and \bar{c} so that we can calculate the spectra of the decay muons. We argue that the distributions calculated from the single gluon-bremsstrahlung mechanism are roughly representative of the $c\bar{c}$ distributions arising from gluon pair production in general, and

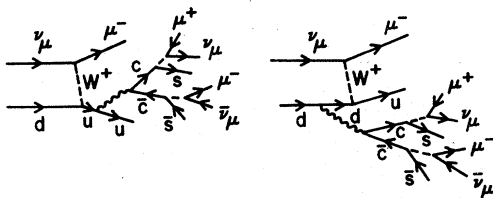


FIG. 5. Feynman diagrams for the neutrino production of a pair of charmed quarks followed by their semileptonic decays.

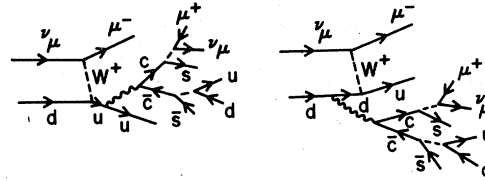


FIG. 6. Feynman diagrams for a $\mu^- \mu^+$ signal from the production and decay of a pair of charmed quarks.

therefore calculate the reduction factor from the neutrino equivalent of Fig. 2. To be specific, the Feynman graphs for $\sigma(\nu_\mu + N \rightarrow \mu^- + c + \bar{c} + X)$, $\sigma(\nu_\mu + N \rightarrow \mu^- + \mu^- + \mu^+ + X)$, $\sigma(\nu_\mu + N \rightarrow \mu^- + \mu^+ + X)$, and $\sigma(\nu_\mu + N \rightarrow \mu^- + \mu^- + X)$ are shown in Figs. 4-7. The actual calculations will be described in the next section. We assume that the muons must have an energy larger than 4 GeV before they can be detected and ignore any angular cut (which is not important for the CDHS and FHPRW experiments). The secondary muons produced when the charmed particles decay tend to be very soft and, although there are small changes due to different choices for fragmentation functions, we find that the detection efficiency is approximately $\frac{1}{3}$ for dimuons and $\frac{1}{10}$ for trimuons. The multimMuon rates are given in Table I assuming that the semileptonic branching ratio is 10%.

Both the final dimuon and trimuon rates are compatible with the latest experimental numbers from the CDHS and FHPRW groups. The $\mu^- \mu^-$ rate will be decisive because we predict $\sigma(\mu^- \mu^-) / \sigma(\mu^- \mu^+) \sim 2\%$, while the FHPRW and CDHS groups quote $(10 \pm 6)\%$ and $(5 \pm 3)\%$, respectively. A more thorough discussion will be given later. However, we must remember that there is also an overflow of misidentified trimuon events into the $\mu^- \mu^-$ signal, so the total rate cannot be due to only $c\bar{c}$ production. Once more $\mu^- \mu^-$ events are analyzed it will be possible to make more definitive statements. If the $\mu^- \mu^-$ event rate goes down, then either our assumption that $\sigma(c\bar{c})/\sigma(\mu^-) = 5 \times 10^{-3}$ will have to be modified or our calculation of the detection efficiency via Figs. 4-7 is incorrect.

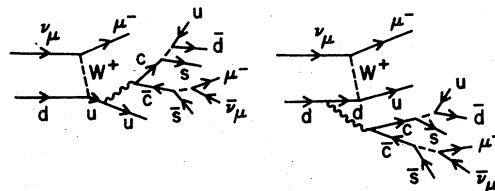


FIG. 7. Feynman diagrams for a $\mu^- \mu^-$ signal from the production and decay of a pair of charmed quarks.

TABLE I. Rates for multimueons produced via $c\bar{c}$ decays. $\sigma(\mu)$ and $\sigma(2\mu) = \sigma(\mu^-\mu^+)$ refers to either the neutrino or antineutrino cross section, respectively. We take $\sigma(\mu^-\mu^+)/\sigma(\mu^-) = \sigma(\mu^+\mu^-)/\sigma(\mu^+) = 1\%$ for the measured dimuon rate arising from single-charmed-particle production.

	ν beam	$\bar{\nu}$ beam
$\sigma(\mu^-\mu^+)/\sigma(\mu)$	$\sim 2 \times 10^{-4}$	
$\sigma(\mu^-\mu^-)/\sigma(\mu)$	$\sim 2 \times 10^{-4}$	
$\sigma(\mu^+\mu^+)/\sigma(\mu)$		$\sim 2 \times 10^{-4}$
$\sigma(\mu^-\mu^-)/\sigma(2\mu)$	$\sim 2 \times 10^{-2}$	
$\sigma(\mu^+\mu^+)/\sigma(2\mu)$		$\sim 2 \times 10^{-2}$
$\sigma(\mu^-\mu^-\mu^+)/\sigma(\mu)$	$\sim 5 \times 10^{-6}$	
$\sigma(\mu^+\mu^-\mu^+)/\sigma(\mu)$		$\sim 5 \times 10^{-6}$

The latter conclusion is unlikely because the same-sign dimuon distributions calculated from the $c\bar{c}$ bremsstrahlung model are very similar to the distributions calculated by Bletzacker *et al.* from a diffractive production model. This shows that the precise nature of the production cross section is unimportant because large regions of phase space are eliminated by the experimental cuts.

III. CALCULATION OF $c\bar{c}$ PRODUCTION AND DECAY

We now outline our calculation of $c\bar{c}$ production from gluon bremsstrahlung^{15,16} as depicted in Fig. 4. The actual work is reasonably straightforward as we can use our previous computer programs for the electromagnetic production of trimuons in neutrino collisions.²³ It is only necessary to change some coupling constants and masses. We assume that the mass of the charmed quark is $m_c = 1.5$ GeV/ c^2 . The x distributions for the valence quarks are again taken to be

$$xu(x)_{\text{val}} = 1.74 \sqrt{x} (1-x)^3 (1+2.3x) \quad (3.1)$$

and

$$xd(x)_{\text{val}} = 1.11 \sqrt{x} (1-x)^{3.1}. \quad (3.2)$$

Even though we know that the absolute cross section calculated from Fig. 4 is too small, the ratios between multimueon rates are probably correct. The gluon coupling constant is optimistically taken to be $\alpha_s = 0.4$. If we now calculate the production process at a fixed energy $E_\nu = 100$ GeV, then $\sigma(c\bar{c}) = 0.8 \times 10^{-40}$ cm², and $\sigma(c\bar{c})/\sigma(\mu^-) \approx 6 \times 10^{-5}$. The corresponding rates for the FHPRW quadrupole triplet (QT) spectrum are $\sigma(c\bar{c}) = 1.0 \times 10^{-40}$, $\sigma(c\bar{c})/\sigma(\mu^-) = 2 \times 10^{-4}$, and for the CDHS 350-GeV wide-

band neutrino beam (WBB) are $\sigma(c\bar{c}) = 0.8 \times 10^{-41}$, $\sigma(c\bar{c})/\sigma(\mu^-) \approx 4 \times 10^{-5}$. The latter rate is very small because the spectrum from the WBB is much softer than the QT spectrum. A comparison of the spectra is given in Ref. 24. The $c\bar{c}$ production cross section rises very rapidly through the energy region of interest, so the QT rate is six times larger than the WBB rate. These numbers need to be multiplied by two branching ratios of 10% each for c and \bar{c} semileptonic decays²⁵ and will still be reduced dramatically by the effects of cuts on the decay muon energies. Thus, the final numbers for the rates turn out to be of the order of 2×10^{-7} for the FHPRW experiment and 0.4×10^{-7} for the CDHS experiment. The latest experimental numbers^{12,14} are $(9 \pm 5) \times 10^{-5}$ and 3×10^{-5} , respectively, so our results are too small to be of experimental importance. Note that adding a cut at say $E = 100$ GeV increases the theoretical trimuon relative rates by approximately a factor of 3 because the $c\bar{c}$ cross section is rising very rapidly in this region of E_ν .

The low value for the rate of associated charm production and decay has led the experimental groups to neglect it as a potential source of trimuon events. We take the viewpoint that we do not understand the dynamics of $c\bar{c}$ production and decay and, in this section, would rather try to work backwards, using the data to get an upper bound on the associated charm-production cross section.

We should now add some comments on the calculation of the complete trimuon process depicted in Fig. 5. Our basic assumption, that the transition from a charmed quark to a charmed hadron is governed by a fragmentation function $D(z)$, which is flat in $z = E_{\text{had}}/E_{\text{quark}}$, follows from the work of Odorico.³ Then the charmed hadron decays via a three-body β decay of the $V-A$ type, i.e., $c \rightarrow s + \mu^+ + \nu_\mu$ and $\bar{c} \rightarrow \bar{s} + \mu^- + \bar{\nu}_\mu$. Previous studies we have made involving heavy-lepton and heavy-quark decays have shown that helicity assumptions can be changed rather radically with negligible changes in the final answers.²⁶ The reason is that the cuts on the muon energies and angles together with the smearing induced by folding the cross section with the neutrino spectrum wash out the small effects due to changes in helicity. We further assume that the mass of the strange quark is 0.4 GeV/ c^2 . The effects of changing our form for $D(z)$ will be discussed in the next section. Note that we have neglected any p_\perp dependence inherent in the fragmentation process.

When one \bar{c} or c quark decays hadronically, as shown in Figs. 6 and 7, we find a dimuon signal, either of the $\mu^-\mu^+$ or of the $\mu^-\mu^-$ type, respectively. However, this is not the only way to make

dimuons. The energy cuts on the trimuon events are very severe so there is a large probability that one muon in the trimuon chain does not survive the cut yielding a dimuon signal. Our calculations indicate that the trimuon rate, when one muon energy is below 4 GeV, is larger than the actual trimuon rate when all muons have energies above 4 GeV. For simplicity let us use the notation that extra parentheses around a muon means that it is below the energy cut. Hence, $\sigma(\mu^-\mu^-(\mu^+))$ denotes the $\mu^-\mu^-$ cross section arising from misidentified trimuon events. Under these circumstances we find that $\sigma(\mu^-\mu^-(\mu^+))/\sigma(\mu^-\mu^-\mu^+)=1.2$ for the FHPRW acceptance, while for the CDHS acceptance this ratio = 1.5. Such effects are expected to be large in any model which produces very-low-energy secondary muons. Thus, the actual $\mu^-\mu^-$ production rate from $c\bar{c}$ decay should be written as

$$\frac{\sigma(\mu^-\mu^-)}{\sigma(\mu^-\mu^-\mu^+)} = \frac{\sigma(\mu^-\mu^-)B_2 + \sigma(\mu^-\mu^-(\mu^+))B_1}{\sigma(\mu^-\mu^-\mu^+)B_1}, \quad (3.3)$$

where B_1 is the branching ratio $\Gamma(c \rightarrow s + \mu^+ + \nu_\mu)/\Gamma(c \rightarrow \text{all})$, and B_2 is the branching ratio for $\Gamma(c \rightarrow s + u + \bar{d})/\Gamma(c \rightarrow \text{all})$. In the counter experiments the electron decay is registered as a hadronic mode so, to a good approximation $B_2 = (1 - B_1) = 0.9$.

The result of our calculation of the diagrams in Figs. 4-7 which includes cuts, spectra and selection criteria for the leading negative muon is that $\sigma(\mu^-\mu^-)$ is approximately twice as large as $\sigma(\mu^-\mu^-(\mu^+))$ so the first term in the numerator of Eq. (3.3) dominates over the second. Thus, the relative dimuon event rates which are independent of the $c\bar{c}$ production cross sections are $\sigma(\mu^-\mu^-)/\sigma(\mu^-\mu^-\mu^+) = 21$ for the FHPRW experiment and 24 for the CDHS experiment. The same rates relative to single-muon events are therefore $\sigma(\mu^-\mu^-)/\sigma(\mu^-) \simeq 3 \times 10^{-5}$ and 1×10^{-6} . The latest data^{13,14} from the two groups are that $\sigma(\mu^-\mu^-)/\sigma(\mu^-\mu^+) = (10 \pm 6) \times 10^{-2}$ for FHPRW and equals $(5 \pm 3) \times 10^{-2}$ for CDHS. Thus, $\sigma(\mu^-\mu^-)/\sigma(\mu^-) \sim (10 \pm 6) \times 10^{-4}$ and $(5 \pm 3) \times 10^{-4}$, respectively. Therefore, as expected, the $c\bar{c}$ production mechanism depicted in Figs. 4-7 gives too small a dimuon rate. We have concentrated here on the same-sign dimuon signal because, although the opposite-sign dimuon signal is approximately equal in size, this channel is completely dominated by dimuons arising from single charm production and decay. The $\mu^-\mu^-$ channel only has backgrounds from regular π and K decays.

In Sec. V we present results for dimuon distributions. As we have seen above, the spillover from trimuon events in which one particle does not sur-

vive the cut is approximately $B_1/B_2 = 1/9$ of the rate for genuine dimuon events, where one charmed quark decays via a semileptonic decay mode and the other via a hadronic decay mode. Therefore, we are justified in neglecting contributions from this channel, and we only give distributions for genuine $\mu^-\mu^-$ events.

IV. RESULTS FOR TRIMUONS

We now present the results of our calculations for trimuons from $c\bar{c}$ decay. To first get a feeling for the dynamics of the production and decay, we show both the distributions for the charmed particles and the final muons for a typical neutrino energy of 100 GeV. Spectra, acceptances, selection criteria, etc. will be included later. We begin by making a comparison between the energy, p_\perp and azimuthal correlations for the $c\bar{c}$ pair and their decay muons. In Fig. 8 we show the energy distributions for the charmed particles and for their decay muons, as well as for the leading μ^- . We follow the usual convention that E_1 refers to the leading μ^- , while E_2 and E_3 refer to the non-leading μ^- and μ^+ , respectively. We assume that there is no ambiguity in distinguishing the leading μ^- from the μ^- arising when \bar{c} decays. We also assume a flat fragmentation function. Although the charmed particles carry a significant amount of energy, the final muons are very soft. This feature can be changed slightly by taking a harder fragmentation function. Assuming $D(z) = \delta(z - 1)$ will transfer all the energy of the charmed quark into the charmed hadron. However, in that case

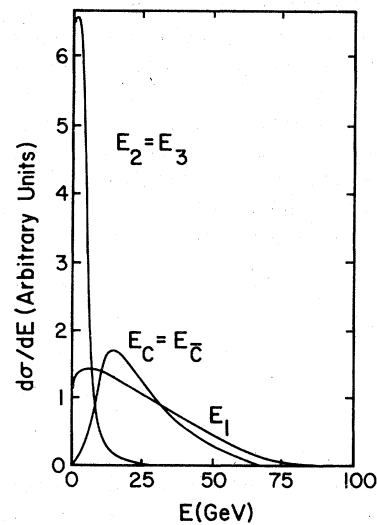


FIG. 8. Energy distributions for E_1 , the leading μ^- , $E_c = E_{\bar{c}}$, the charmed quarks, and $E_2 = E_3$, the non-leading μ^- and μ^+ , respectively.

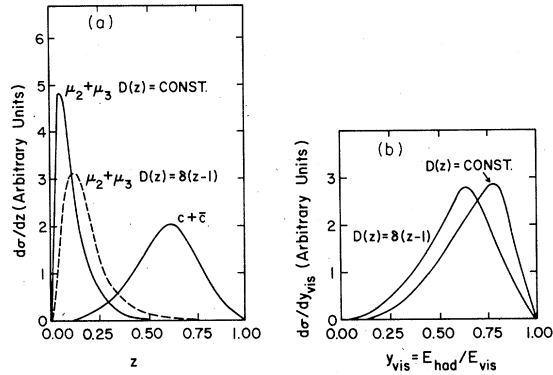


FIG. 9. The distributions in (a) the variable z for the $\mu_2\mu_3$ pair and the $c\bar{c}$ pair and (b) the variable y_{vis} .

we find $\langle E_{\mu^-} \rangle = \langle E_{\mu^+} \rangle = 7$ GeV rather than the previous value of 3.5 GeV.

These features are exhibited rather dramatically in a plot of the variable $z_i = (E_2 + E_3) / (E_{\text{had}} + E_2 + E_3)$. In Fig. 9(a) we plot the distribution in this variable for the cases $D(z) = \text{const}$ and $D(z) = \delta(z-1)$. In the first case z_i is badly peaked for small z_i because some of the hadronic energy comes from the decays of the charmed particles. In the second case the peak in z_i is at a slightly larger value because we have maximized the amount of energy we can feed into the muons and thereby minimized the hadronic energy. We also show the distribution in z_c for the charmed particles, where $z_c = (E_c + E_{\bar{c}}) / (E_{\text{had}} + E_c + E_{\bar{c}})$. This function peaks at $z_c = 0.6$.

There is no ambiguity in the definition of E_{had} . However, if we use variables which involve the beam energy, then we must take this to be E_{vis} on

account of the two missing neutrinos, and $E_{\text{vis}} < E_{\text{beam}}$. Hence, if we define $y_{\text{vis}} = E_{\text{had}} / E_{\text{vis}}$ we find that this variable peaks around 0.6–0.7 because E_{had} is increased by the additional hadronic energy arising from the charmed particle decays, while E_{vis} is reduced by the energy carried away by the two missing neutrinos. This variable is shown in Fig. 9(b) again for the two choices $D(z) = \text{const}$, for which $\langle y_{\text{vis}} \rangle = 0.7$ and $D(z) = \delta(z-1)$ for which $\langle y_{\text{vis}} \rangle = 0.6$. The latter case gives us the lowest possible value for $\langle y_{\text{vis}} \rangle$.

We now turn to the distribution in the invariant mass combinations. Figure 10 shows the invariant masses of the $c\bar{c}$ pair, the nonleading $\mu^- \mu^+$ pair ($\mu_2 \mu_3$) and the invariant masses of the other dimuon combinations. We point out that even though the $\mu_2 \mu_3$ invariant mass is rather small, it does have a long tail reflecting the fact that these muons do not come from a point source. The invariant mass of the $\mu_1(c+\bar{c})$ system as well as that of the $\mu_1 \mu_2 \mu_3$ system are shown in Fig. 11.

We now define a four-vector which is the sum of the four vectors of the charmed quarks and another four-vector which is the sum of the μ_2 and μ_3 four-vectors. These vectors are aligned predominately along the hadron shower (or W -boson) direction defined with respect to the leading μ^- . To show this, we present their perpendicular components along the hadron-shower direction in Fig. 12. The results from our numerical computations show that $\langle p_{\perp} \rangle_{\mu\mu} = 0.6$ GeV/ c , while $\langle p_{\perp} \rangle_{c\bar{c}} = 1.4$ GeV/ c which demonstrates that the final dimuon pair distribution is narrower than that of the $c\bar{c}$ pair.

The final distribution we wish to present here is the azimuthal angle between the leading μ^- and the

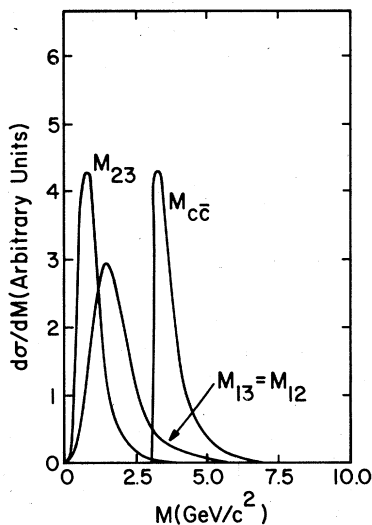


FIG. 10. The invariant-mass distribution for the $c\bar{c}$ pair and the three invariant-mass distributions for the dimuon pairs.

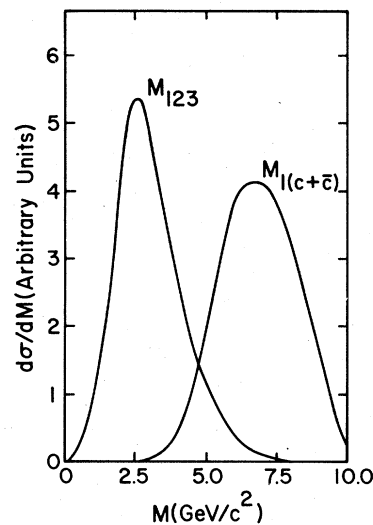


FIG. 11. The invariant-mass distributions for the $\mu_1(c+\bar{c})$ system and the trimuon invariant-mass distribution.

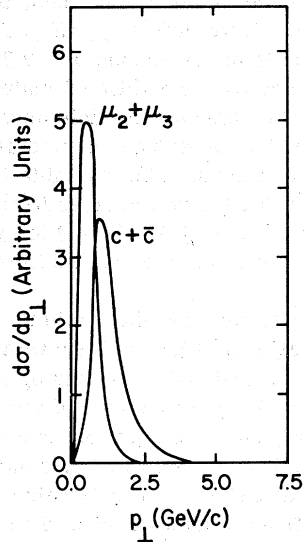


FIG. 12. The transverse-momentum distributions of the $c\bar{c}$ pair and the decay dimuon pair ($\mu_2\mu_3$) along the hadron-shower direction.

sum of the $c\bar{c}$ and/or $\mu_2\mu_3$ vectors projected on a plane perpendicular to the neutrino direction.

Figure 13 shows this distribution as well as those for the azimuthal angles between the three pairs of muons, i.e., $\mu_1\mu_2$, $\mu_1\mu_3$, and $\mu_2\mu_3$. One important observation we can make from this plot is that the ϕ distribution for the $\mu_1(c+\bar{c})$ system is sharply peaked in the backward direction demon-

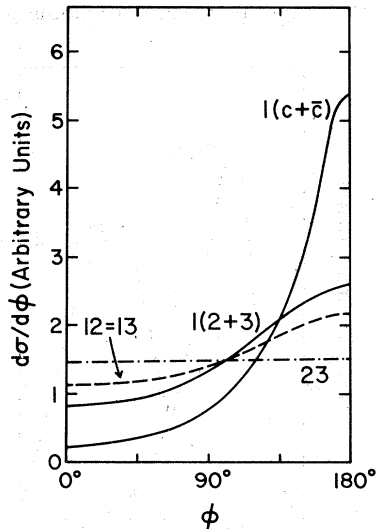


FIG. 13. The azimuthal angular distributions with respect to the neutrino beam direction between leading μ^- and the dicharm system ($c+\bar{c}$ pair) and dimuon system (nonleading $\mu^- \mu^+$ pair), respectively. Also shown are the azimuthal angular distributions between the three dimuon pairs $\mu_1\mu_2$, $\mu_2\mu_3$, and $\mu_1\mu_3$.

strating that the transverse momentum vector of the $(c+\bar{c})$ system is oppositely aligned to that of the original μ^- . This follows from the conservation of transverse momentum in the initial interaction. However, after the charmed particles have decayed, the final muons are not so sharply aligned, and the ϕ distribution between μ_1 and $(\mu_2+\mu_3)$ is therefore much flatter. We will exploit this fact in our later analysis. The distributions we have given above show specific features which we have extracted as particularly relevant to the $c\bar{c}$ production process. Other distributions which we have examined are not too informative. Note that if we change the fragmentation function from $D(z) = \text{const}$ to $D(z) = \delta(z-1)$, then there are only small changes in the p_{\perp} distributions for the final muons and in the ϕ plots, whereas there are large changes in the z and y_{vis} plots.

We now give results for both the CDHS experiment and the FHPRW experiment, taking into account their different selection criteria, cuts, and spectra. Out of the 76 events found by the CDHS collaboration, 63 were discovered in the 350-GeV WBB and 13 in the 400-GeV WBB. The FHPRW group are presently analyzing the results of a new run using the 400-GeV QT beam at Fermilab and expect to have a comparable number of events. We remind the reader that the CDHS experiment is most sensitive to neutrino energies around 100 GeV, while the FHPRW experiment has a harder neutrino spectrum and is most sensitive to neutrino energies around 180 GeV.

The selection criterion for the leading μ^- is different between the two experiments. The FHPRW group choose the leading μ^- to be the faster of the μ^- particles measured in the trimuon events. The CDHS group choose the following definition of the leading μ^- . Take one μ^- , define from it a W -boson direction and add the two values of the transverse-momentum components of the other muons along this direction. Then repeat the analysis with the other μ^- . The case where the sum is a minimum is then chosen to define the secondary pair and therefore the leading muon. We will use this selection criterion when we perform a Monte Carlo calculation of the distributions for the CDHS events. For the case of the FHPRW events we use their definition of the leading muon. Cuts are incorporated such that the muon energies must be larger than 4.0 GeV for both experiments. One additional complication which must be faced is that the CDHS data show the presence of an electromagnetic source for some of their trimuon events.¹² In particular, the events at small $\phi_{1(2+3)}$ are compatible with Dalitz production of a muon pair off the leading μ^- . Fifteen events are of this type and nine survive an additional cut that all three muons have

at least $0.2\text{-GeV}/c$ transverse momentum with respect to the neutrino direction. This latter cut is applied to remove those events whose $\phi_{1(2+3)}$ angle is difficult to measure. Accordingly, we should remove nine events from the $\phi_{1(2+3)}$ plot and 15 from the other plots. Rather than discard these events we show them with dashed lines. The net result is that the histogram for $\phi_{1(2+3)}$ has sixty events, while the other histograms have 76. In order to reduce somewhat the number of plots, we only present distributions which help to distinguish the presence of a $c\bar{c}$ signal.

Let us start by comparing our distributions with the CDHS results. We fold in their neutrino spectrum, employ their cuts and selection criteria, and present our theoretical results for the complete decay chain shown in Fig. 5. In Fig. 14(a) we show the plot of the nonleading-dimuon invariant-mass distribution versus the CDHS data. The area under the solid curve has been normalized to the nonelectromagnetic events, and it is obvious that the model does not fit the large peak at small values of M_{23} . Figure 14(b) shows the prediction for the FHPRW experiment. In Fig. 15(a) we show the p_{\perp} distribution for the nonleading dimuon pair projected along the hadron-shower direction. This direction is defined using E_{vis} for the neutrino energy because we lose energy into the two missing neutrinos. Two electromagnetic events have $p_{\perp} \sim 4.6\text{ GeV}/c$. We have compiled the data points from a listing of the CDHS results, and there are small discrepancies between this histogram and the previous versions referred to in Ref. 12. The $c\bar{c}$ model fits this p_{\perp} distribution reasonably well. In Fig. 15(b) we present the results for the FHPRW distribution. Figure 16(a) shows the ϕ distribution between the leading μ^{-} and the sum of the other muon momenta. In accord with the CDHS analysis we have added an extra cut (only for this plot) to eliminate all events where the transverse momenta of all muons with respect to the neutrino beam direction is less than $0.2\text{ GeV}/c$. The events at

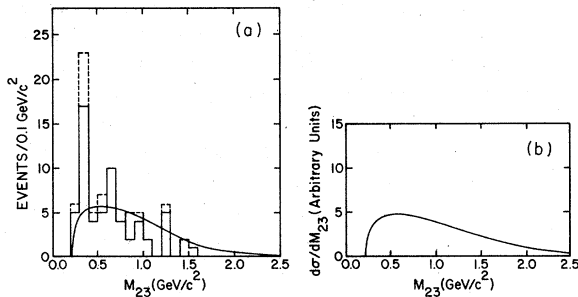


FIG. 14. The theoretical prediction of the nonleading dimuon invariant mass for (a) the CDHS experiment, and (b) the FHPRW experiment.

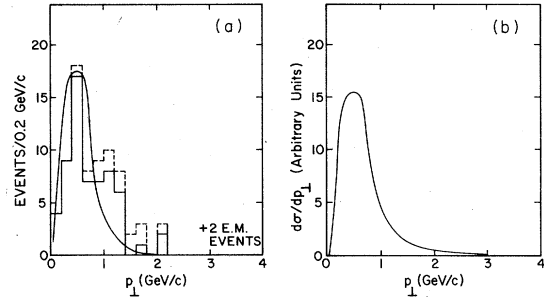


FIG. 15. The P_{\perp} distribution for the sum of the non-leading dimuon pair for (a) the CDHS experiment and (b) the FHPRW experiment.

small $\phi_{1(2+3)}$ are the electromagnetic events we mentioned previously. Clearly the $c\bar{c}$ model cannot explain the large peak near 180° . If we normalize the theoretical prediction by the events at 90° , then the signal from a $c\bar{c}$ production mechanism cannot account for more than approximately 50% of the events at large ϕ . These particular events are given a "hadronic" interpretation by the CDHS group because they are similar in nature to the dimuon events seen in the reactions $\pi + p \rightarrow \mu^{+} + \mu^{-} + X$ and $p + p \rightarrow \mu^{+} + \mu^{-} + X$. Our prediction for the FHPRW ϕ distribution is given in Fig. 16(b).

In Fig. 17(a) we show the distribution in the variable z_1 defined above. The individual muon energy distributions are very sharply peaked at small values, leading to a z_1 distribution which peaks at $z_1 = 0.2$. The data, however, show a much flatter distribution so only 40% of the CDHS events can be compatible with the $c\bar{c}$ production model. In Fig. 17(b) we show the predicted z_1 distribution for the FHPRW events. Figure 18(a) shows the distribution in $y_{\text{vis}} = E_{\text{had}}/E_{\text{vis}}$ for the $c\bar{c}$ model. The corresponding CDHS data do not show an enhancement around $y_{\text{vis}} = 0.75$. If we take this distribution then the total amount of $c\bar{c}$ associated production allowed in the CDHS data is approximately 20%.

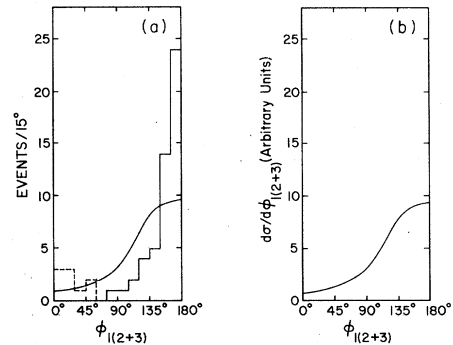


FIG. 16. The $\phi_{1(2+3)}$ distribution for (a) the CDHS experiment and (b) the FHPRW experiment.

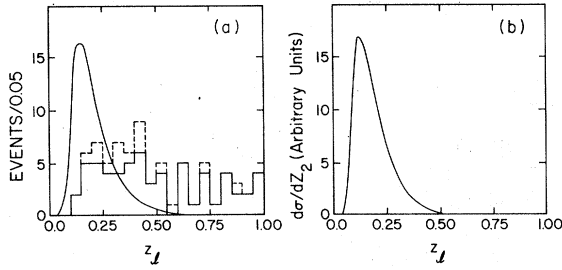


FIG. 17. The z_2 distribution for (a) the CDHS experiment and (b) the FHPRW experiment.

The prediction for the FHPRW data is shown in Fig. 18(b). Finally, we show for completeness the distribution in $x = Q^2/2M\nu_{\text{vis}}$ in Fig. 19(a). The data favor a lower average value for x , indicating that the $c\bar{c}$ production takes place off valence quarks and the average x is around 0.22. This average is slightly reduced for the FHPRW experiment as shown in Fig. 19(b). It is interesting to compare the results given in Figs. 9, 10, 12, and 13 at fixed beam energy with those shown in Figs. 14–17.

A short study of Figs. 14–19 is enough to convince anyone that the associated production model is inconsistent with the bulk of the CDHS data, and therefore can only comprise a small fraction of the event rate. Insofar as we have a realistic model for the $c\bar{c}$ production and decay, we can use the distributions to conclude that this mechanism cannot comprise more than 40% of the total trimuon rate or $\sigma(\mu^-\mu^-\mu^+)/\sigma(\mu^-) \leq 1 \times 10^{-5}$. In fact, this number is a rather generous estimate because the y_{vis} plot indicates an even smaller signal. However, we can change the y_{vis} distribution by changing the fragmentation function to $D(z) = \delta(z-1)$ and make it peak at slightly smaller y_{vis} so we consider the 40% limit a safe one. The main defects of the $c\bar{c}$ model is that it cannot account for those events which have very small dimuon masses and are sharply collimated along the hadron beam direction so that $\phi_{1(2+3)} \simeq 180^\circ$. The FHPRW trimuon rate from $c\bar{c}$ production and decay could be as

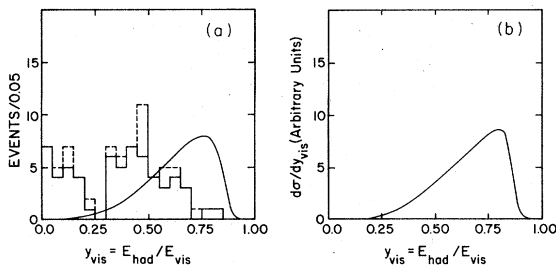


FIG. 18. The distribution in $y_{\text{vis}} = E_{\text{had}}/E_{\text{vis}}$ for (a) the CDHS experiment and (b) the FHPRW experiment.

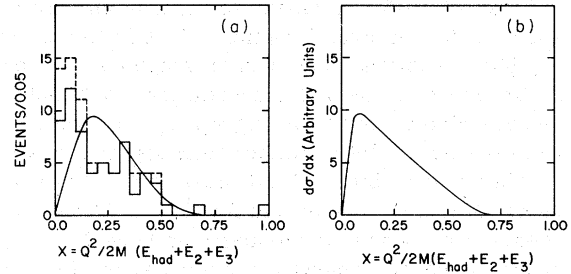


FIG. 19. The distribution in $x = Q^2/2M(E_{\text{had}} + E_2 + E_3)$ for (a) the CDHS experiment and (b) the FHPRW experiment.

large as 4×10^{-5} of the single-muon inclusive cross section if we scale by the same factor as in Sec. III. A more refined treatment will be possible when their new data are available.

V. RESULTS FOR DIMUONS

We now turn our attention to dimuon signals from the production and decay of $c\bar{c}$ pairs. There are two questions which need to be addressed, namely the size of the $\mu^-\mu^+$ signal and the size of the $\mu^-\mu^-$ signal. The former process arises directly when the \bar{c} decays hadronically while the c decays semileptonically, as in Fig. 6; while the latter arises directly when the c decays semileptonically and the \bar{c} decays hadronically, as in Fig. 7. Both processes also occur when one of the soft muons in the trimuon reaction is eliminated by the minimum energy cut.

The calculation of these decay chains follows easily from the programs used in our previous work. The dimuon event rates are essentially equal apart from a small correction factor associated with the $\mu^-\mu^-$ events. Relative to the trimuon event rate, the dimuon event rate is enhanced by the branching ratio for hadronic decay relative to semileptonic decay and the effects of dimuon versus trimuon acceptance. As we have seen above, our trimuon rate is too low to explain the trimuon events. Nevertheless, relative branching ratios are likely to be correct because our programs do include the important effects due to the limited detector acceptance. If we assume that the upper limit on the CDHS trimuon event rate via $c\bar{c}$ production and decay is $\sigma(\mu^-\mu^-\mu^+)/\sigma(\mu^-) = 1 \times 10^{-5}$ as found in the last section, then the dimuon event rate could be as large as $\sigma(\mu^-\mu^-)/\sigma(\mu^-) = 2.4 \times 10^{-4}$ leading to $\sigma(\mu^-\mu^-)/\sigma(\mu^-\mu^+) \sim 2 \times 10^{-2}$. The number for the FHPRW experiment is probably around three times larger due to their harder neutrino spectrum. These numbers are compatible with the latest experimental results of $(5 \pm 3)\%$ and

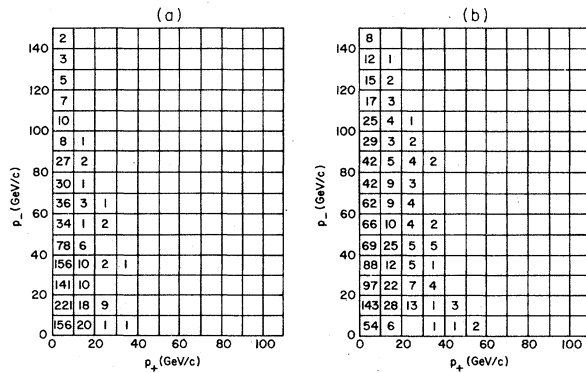


FIG. 20. Scatter plot of the energies of the $\mu^- \mu^+$ events for (a) the CDHS experiment and (b) the FHOPRW experiment. The numbers are normalized to approximately 1000 events.

(10 ± 6)%.

Our results from Sec. II imply an expected rate of $\sim 5 \times 10^{-6}$ for $\sigma(\mu^- \mu^- \mu^+) / \sigma(\mu^-)$ and $\sim 2 \times 10^{-2}$ for $\sigma(\mu^- \mu^-) / \sigma(\mu^- \mu^+) [= \sigma(\mu^- \mu^+ \text{ from } c\bar{c}) / \sigma(\mu^- \mu^+)]$. These are consistent with the upper bounds we found from the trimuon distributions. We now have to examine the distributions for the dimuon events to see if a $c\bar{c}$ signal can be extracted from the large background due to π and K decays. To reduce these backgrounds it will probably be necessary to increase the minimum energy requirement on the muons. Also, we should state here that CDHS criterion for the leading μ^- is applied for their $\mu^- \mu^-$ events, namely, that the leading μ^- has the larger p_\perp along the W -boson direction. The FHPRW events are ordered according to their energy so the leading μ^- is the faster of the two.

We show momentum scatter plots for the $\mu^- \mu^+$ and $\mu^- \mu^-$ events for the CDHS and FHPRW experi-

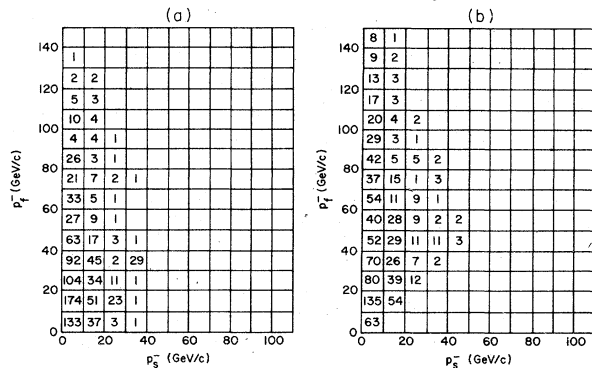


FIG. 21. Scatter plot of the energies of the $\mu^- \mu^-$ events for (a) the CDHS experiment and (b) the FHOPRW experiment. The numbers are normalized to approximately 1000 events.

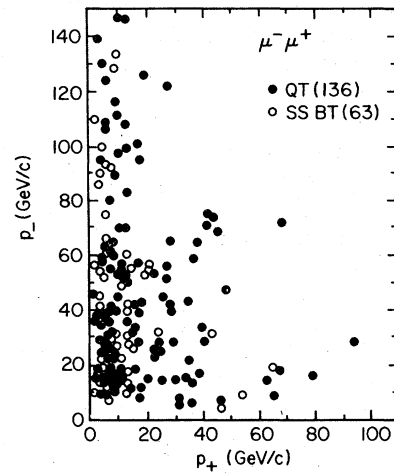


FIG. 22. Scatter plot for the energies of the FHOPRW $\mu^- \mu^+$ events.

ments in Figs. 20 and 21. In the case of the $\mu^- \mu^-$ plots we use the notation p_f for the fast-muon momentum in the FHPRW case and the leading-muon momentum for the CDHS case. The other particle momentum is denoted by p_s . We see in Fig. 21(a) that the CDHS choice does not throw all the events above the diagonal $p_f = p_s$ because some of their leading muons are not the faster of the two.

The latest available data from the FHPRW experiment (now called FHOPRW to include Ohio State) is shown in Figs. 22 and 23. These plots are taken from the talk of Ling,¹⁴ and include both data from the QT beam at Fermilab as well as the bare-target sign-selected beam at Fermilab. The beams are similar in shape so we are justified in comparing our results in Fig. 20(b) and 21(b) with the data. We see from these plots that it will be

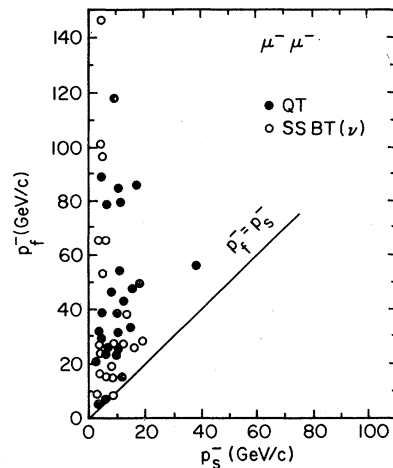


FIG. 23. Scatter plot for the energies of the FHOPRW $\mu^- \mu^-$ events.

practically hopeless to extract any signal from the $\mu^- \mu^+$ events because the scatter plot is so similar in shape to the data which we know is explained by single charm excitation and decay.

The $\mu^- \mu^-$ plot looks more hopeful. So long as energetic dimuons from π and K decays can be suppressed and some events remain in the so-called symmetric region (large p_f and p_s), then a $c\bar{c}$ explanation remains a possibility. This is a very difficult experimental problem. Some of the tests given by Albright and Smith²⁷ to try to distinguish heavy leptons and squarks from regular charm decay can possibly be exploited here.

Now we turn our attention to the transverse momentum distributions along the W -boson direction (defined with respect to the leading muon for CDHS and the fast muon for FHOPRW). The p_\perp spectra for the nonleading μ^- and for the μ^+ are shown in Fig. 24(a) for the $\mu^- \mu^-$ and $\mu^- \mu^+$ events in the CDHS experiment. The actual data from the FHOPRW group are compared with our predictions in Fig. 24(b).

Another interesting quantity to examine is the opening angle between the dimuons projected on a plane perpendicular to the neutrino beam. This azimuthal angle peaks near 180° for the $\mu^- \mu^+$ events because the charmed particle tends to follow the hadronic direction. In Fig. 25(a) we show our results for the CDHS experiment for both the $\mu^- \mu^-$ and $\mu^- \mu^+$ events. The corresponding distributions are given in Fig. 25(b) for the FHOPRW experiment where we also add the latest data.

It is obvious from Figs. 21, 23, and 24 that the $\mu^- \mu^-$ events seen by the FHOPRW group are compatible with the theoretical predictions from $c\bar{c}$ decay. However, these are not the best variables to examine to isolate a $c\bar{c}$ component. We would like to propose that the variables $z_1 = E_2/(E_{\text{had}} + E_2)$ and $y_{\text{vis}} = E_{\text{had}}/E_{\text{vis}}$ are more convenient for this purpose.

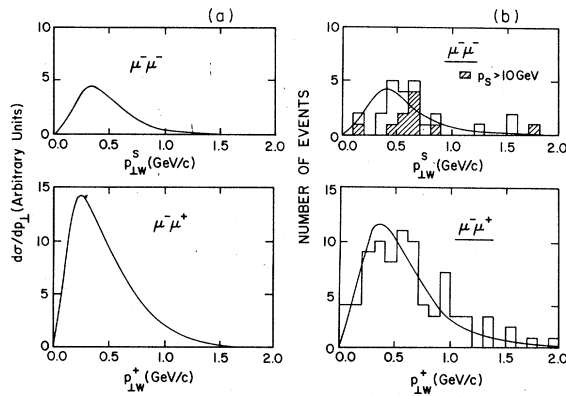


FIG. 24. Muon p_\perp distributions for the $\mu^- \mu^+$ and $\mu^- \mu^-$ events in (a) the CDHS experiment and (b) the FHOPRW experiment.

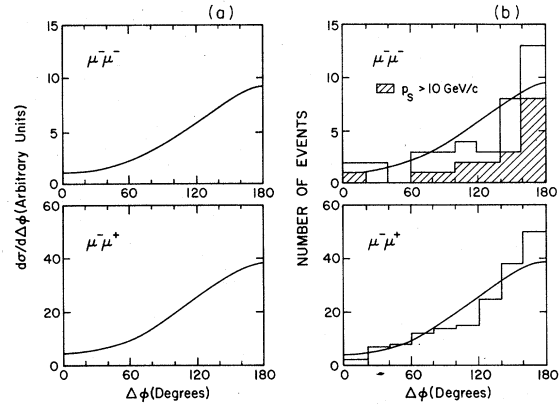


FIG. 25. Azimuthal angular distributions between the muons for the $\mu^- \mu^+$ and $\mu^- \mu^-$ events in (a) the CDHS experiment and (b) the FHOPRW experiment.

As we discussed in Sec. IV the fact that there is at least one missing neutrino, means that E_2 is small and E_{had} is larger than expected owing to the additional hadronic energy from the decay of the charmed particle. Hence, z_1 peaks near zero as in Fig. 17. Similarly, y_{vis} peaks near unity as in Fig. 18 because E_{had} is increased and E_{vis} is diminished when the \bar{c} decays relative to their values in the basic production process. As more data are collected, it will be possible to try these tests for different cuts in the energy of the second μ^- .

VI. CONCLUSIONS

We have examined the possibility that $c\bar{c}$ production and decay can lead to some of the dimuon and trimuon events seen in the CDHS and FHPRW experiments. The reason for undertaking this project is that the cross section for the associated production of charmed particles seems to be rather large in hadronic interactions and in photoproduction.^{17,18} Because of our present lack of understanding of charm production we have to base our analysis on a model. For definiteness we assume that the gluon-bremsstrahlung model is adequate to describe the distributions even though its rate is too small to explain the magnitude of the experimental signal.^{15,16} This assumption has some degree of validity because our distributions are remarkably similar to those calculated previously by Bletzacker, Nieh, and Soti¹⁰ and their approach was entirely different from ours. Other possible mechanisms will also produce $c\bar{c}$ in similar kinematical regions. We therefore conclude that the experimental acceptances are so severe that large regions of phase space are unimportant. Thus, the behavior of the production matrix element in those regions is not very important.

The kinematics of the production reaction is such that the relatively heavy $c\bar{c}$ pairs are produced at some small p_{\perp} with respect to the hadron-shower direction carrying a reasonable fraction of the neutrino-beam energy. When they decay via a semileptonic mode then the final muons only receive a small fraction of the energy and, at the same time, become more uniformly distributed in p_{\perp} . By the time we smear this cross section by the energy spectrum, the distributions in the azimuthal angles between the muons are very flat. Actually we regain some peaking by adding 4-GeV energy cuts on all the muons because the fast ones tend to follow the hadron shower direction. The resulting $\phi_{1(2+3)}$ distribution is much flatter than the $\phi_{1(c+\bar{c})}$ distribution. Similarly the distribution in z_l is peaked at $z_l \approx 0.2$, while that for z_c is peaked at $z_c \approx 0.6$. The peaking in $y_{\text{vis}} = E_{\text{vis}}/E_{\text{had}}$ near unity is another characteristic feature.

A careful study of the CDHS data now shows that the ϕ , z_l , and y_{vis} distributions cannot allow a large signal from $c\bar{c}$ production and decay. The mechanism responsible for "hadronic" trimuons must produce dimuon systems which carry a reasonable fraction of the hadronic energy and be sharply aligned along the hadron shower direction. Using the experimental data we conclude that $c\bar{c}$ production can at most account for 40% of the CDHS events so that the upper bound on $\sigma(\mu^-\mu^-\mu^+)/\sigma(\mu^-)$ is approximately 1×10^{-5} when we exclude the known electromagnetic signal which contributes for small $\phi_{1(2+3)}$. This number can be changed slightly by varying the fragmentation function for the charmed quarks but even in the extreme case of $D(z) = \delta(z-1)$, i.e., where the charmed hadron carries all the energy of the quark, the $c\bar{c}$ model cannot possibly explain more than 50% of the data.

We then studied the production of dimuon pairs from the processes where one of the charmed particles decays hadronically, leading to $\mu^-\mu^+$ and $\mu^-\mu^-$ signals. Unfortunately, the $\mu^-\mu^+$ signal is not very easy to observe because of the large rate in this channel from single-charm production and decay. Concentrating therefore on the $\mu^-\mu^-$ events,

we examined the distributions in their momenta, p_{\perp} components along the hadron-shower direction and azimuthal opening angles. In general the recent FHOPRW data are in agreement with our predictions from the $c\bar{c}$ production model. Hence, if the rate for $c\bar{c}$ production is sufficient to explain approximately one half of the trimuon events, we conclude that event rates as large as 2–8% can be expected for $\sigma(\mu^-\mu^-)/\sigma(\mu^-\mu^+)$. One possible way to eliminate the $c\bar{c}$ model as an explanation of the $\mu^-\mu^-$ events is to exploit the distributions in z_l and y_{vis} . It will take much more data before the presence of a real signal can be positively extracted from the backgrounds from π and K decay.

Proceeding in a different direction, in Sec. II we argued that the expected size of $c\bar{c}$ production in ν reactions could be estimated starting from data on photoproduction of the J/ψ . This leads us to expect that $c\bar{c}$ production accounts for about $\frac{1}{5}$ of the trimuon signal and most of the opposite-sign dimuon signal. These results are consistent with the limits derived from the analysis of the dimuon and trimuon events. Therefore, the associated production of $c\bar{c}$ pairs with a rate approximately $\frac{1}{2}\%$ of the total neutrino inclusive cross section is compatible with present data. Any reduction of the $\mu^-\mu^-$ signal will cause a corresponding reduction of the $c\bar{c}$ rate. The precise nature of the $c\bar{c}$ production mechanism needs further study. We conclude that there is no need to propose any exotic explanations for a same-sign dimuon signal.

ACKNOWLEDGMENTS

This work was supported in part by the National Science Foundation under Grant No. PHY 76-15328 and by the Department of Energy. J. Smith would like to thank C. H. Albright, H. T. Nieh, and M. Paschos for profitable discussions. He would also like to acknowledge discussions with members of the CDHS and FHOPRW groups, in particular with K. Kleinknecht, J. Knobloch, T. Y. Ling, A. K. Mann, D. Schlatter, and R. Turlay.

¹S. L. Glashow, J. Iliopoulos, and L. Maiani, Phys. Rev. D **2**, 1285 (1970).

²M. Holder *et al.*, Phys. Lett. **69B**, 377 (1977).

³R. Odorico, Phys. Lett. **71B**, 121 (1977). R. Odorico and V. Roberto, Nucl. Phys. **B136**, 333 (1978).

⁴C. H. Lai, Phys. Rev. D **18**, 1422 (1978).

⁵C. Baltay *et al.*, Phys. Rev. Lett. **39**, 62 (1977).

⁶Preliminary data are already available on $K\pi\pi$ final states from the Columbia-BNL experiment at Fermilab. For a summary of the hadronic production data see C. Baltay, in *Neutrinos—78*, proceedings of the International Conference on Neutrino Physics and Astro-

physics, Purdue University, edited by Earle C. Fowler (Purdue University, Lafayette, Indiana, 1978).

⁷B. C. Barish *et al.*, Phys. Rev. Lett. **38**, 577 (1977).

⁸A. Benvenuti *et al.*, Phys. Rev. Lett. **38**, 1110 (1977); **38**, 1183 (1977); **40**, 432 (1978); **40**, 488 (1978). See also talk by D. Reeder, in *Proceedings of the International Symposium on Lepton Interactions at High Energies, Hamburg, 1977*, edited by F. Gutbrod (DESY, Hamburg, 1977), p. 259.

⁹M. Holder *et al.*, Phys. Lett. **70B**, 393 (1977).

¹⁰F. Bletzacker, H. T. Nieh, and A. Soni, Phys. Rev. Lett. **38**, 1241 (1977); F. Bletzacker and H. T. Nieh,

State University of New York at Stony Brook Report No. ITP-SB-77-42 (unpublished).

- ¹¹F. Bletzacker, H. T. Nieh, and A. Soni, *Phys. Rev. Lett.* **37**, 1316 (1976); F. Bletzacker and H. T. Nieh, State University of New York at Stony Brook Report No. ITP-SB-77-44 (unpublished).
- ¹²T. Hansl *et al.*, CERN reports, 1978 (unpublished). See also K. Kleinknecht, in *New Frontiers in High-Energy Physics*, proceedings of Orbis Scientiue 1978, edited by Arnold Perlmutter and Linda F. Scott (Plenum, New York, 1978); talk at the XIIIth Rencontre de Moriond (unpublished); D. Schlatter, in *New Results in High Energy Physics—1978*, proceedings of the Third International Conference at Vanderbilt University, edited by R. S. Panvini and S. E. Csorna (AIP, New York, 1978); J. Knobloch, in *Neutrinos—78* (Ref. 6).
- ¹³M. Holder *et al.*, *Phys. Lett.* **70B**, 396 (1977).
- ¹⁴T. Y. Ling, paper presented at the XIIIth Rencontre de Moriond, 1978 [Ohio Univ. State Report No. COO-1545-232, 1978 (unpublished)].
- ¹⁵H. Goldberg, *Phys. Rev. Lett.* **39**, 1598 (1977).
- ¹⁶B. L. Young, T. F. Walsh, and T. C. Yang, *Phys. Lett.* **74B**, 111 (1978).
- ¹⁷P. Alibrán *et al.*, *Phys. Lett.* **74B**, 134 (1978); T. Hansl *et al.*, *ibid.* **74B**, 139 (1978); P. C. Bosetti *et al.*, *ibid.* **74B**, 143 (1978).
- ¹⁸R. Prepost, in *Proceedings of the 1975 International Symposium on Lepton and Photon Interactions at High Energy*, edited by W. T. Kirk (SLAC, Stanford, 1975), p. 241; R. L. Anderson, in *Proceedings of the International Conference on the Production of Particles with New Quantum Numbers*, edited by D. Cline and J. Kolonko (University of Wisconsin, Madison, Wis., 1976), p. 196; W. Y. Lee, in *Proceedings of the International Symposium on Lepton and Photon Interactions at Energies, Hamburg, 1977*, edited by F. Gutbrod (DESY, Hamburg, 1977), p. 555.
- ¹⁹A careful treatment is given by D. Sivers, J. Town-duction by photons of about $\frac{1}{4} \mu\text{b}$. Since $\sigma_{\text{el}} \ll \sigma_{\text{TOT}}$, the scattering is far from absorptive, and we assume an estimate of 2–4 times the lower bound is quite reasonable.
- ²⁰T. Nash *et al.*, *Phys. Rev. Lett.* **36**, 1233 (1976).
- ²¹L. M. Jones and W. H. Wyld, *Phys. Rev. D* **17**, 759 (1978).
- ²²J. Babcock, D. Sivers, and S. Wolfram, *Phys. Rev. D* **18**, 162 (1978). See also V. A. Vainshtein, and V. I. Zakharov, *Nucl. Phys.* **B136**, 125 (1978), who have discussed sum rules for charm photoproduction within the framework of quantum chromodynamics.
- ²³J. Smith and J. A. M. Vermaseren, *Phys. Rev. D* **17**, 2288 (1978).
- ²⁴J. Smith, in *Neutrinos—78*, (Ref. 6). Some preliminary results from our $c\bar{c}$ calculations were reported at this meeting.
- ²⁵Values for the semileptonic branching ratios of charmed quarks vary between 10% and 15%. See the talks by J. Kirkby, A. Barbaro-Galtieri, S. Yamada, and P. Bloch, in *Proceedings of the International Symposium on Lepton and Photon Interactions at High Energies, Hamburg, 1977*, edited by F. Gutbrod (DESY, Hamburg, 1977), pp. 3, 21, 69, and 293, respectively.
- ²⁶We are referring here to the heavy-lepton cascade decay interpretation of the trimuon events by C.H. Albright, J. Smith, and J.A. M. Vermaseren, *Phys. Rev. Lett.* **38**, 1187 (1977); *Phys. Rev. D* **16**, 3182 (1977); **16**, 3204 (1977); **18**, 108 (1978). See also C. H. Albright, R. E. Shrock, and J. Smith, *Phys. Rev. D* **17**, 2383 (1978).
- ²⁷C. H. Albright and J. Smith, *Phys. Lett.* **77B**, 94 (1978).